Erlotinib (Tarceva, OSI-774) Antagonizes ATP-Binding Cassette Subfamily B Member 1 and ATP-Binding Cassette Subfamily G Member 2–Mediated Drug Resistance

Zhi Shi,[1,2] Xing-Xiang Peng,[1] In-Wha Kim,[3] Suneet Shukla,[3] Qiu-Sheng Si,[5] Robert W. Robey,[4] Susan E. Bates,[4] Tong Shen,[1] Charles R. Ashby, Jr.,[1] Li-Wu Fu,[2] Suresh V. Ambudkar,[3] and Zhe-Sheng Chen[1]

[1]Department of Pharmaceutical Sciences, College of Pharmacy and Allied Health Professions, St. John's University, Jamaica, New York; [2]State Key Laboratory for Oncology in South China, Cancer Center, Sun Yat-Sen University, Guangzhou, China; [3]Laboratory of Cell Biology and [4]Medical Oncology Branch, Center for Cancer Research, National Cancer Institute, NIH, Bethesda, Maryland; and [5]Department of Pathology, Memorial Medical Center, Member Coremaugh Health System, Johnstown, Pennsylvania

Abstract

It has been reported that gefitinib, an epidermal growth factor receptor (EGFR) tyrosine kinase inhibitor (TKI), has the ability to modulate the function of certain ATP-binding cassette (ABC) transporters and to reverse ABC subfamily B member 1 (ABCB1; P-glycoprotein)– and ABC subfamily G member 2 (ABCG2; breast cancer resistance protein/mitoxantrone resistance protein)–mediated multidrug resistance (MDR) in cancer cells. However, it is unknown whether other EGFR TKIs have effects similar to that of gefitinib. In the present study, we have investigated the interaction of another EGFR TKI, erlotinib, with selected ABC drug transporters. Our findings show that erlotinib significantly potentiated the sensitivity of established ABCB1 or ABCG2 substrates and increased the accumulation of paclitaxel or mitoxantrone in ABCB1- or ABCG2-overexpressing cells. Furthermore, erlotinib did not significantly alter the sensitivity of non-ABCB1 or non-ABCG2 substrates in all cells and was unable to reverse MRP1-mediated MDR and had no effect on the parental cells. However, erlotinib remarkably inhibited the transport of $E_2$17βG and methotrexate by ABCG2. In addition, the results of ATPase assays show that erlotinib stimulated the ATPase activity of both ABCB1 and ABCG2. Interestingly, erlotinib slightly inhibited the photolabeling of ABCB1 with [^{125}I] iodoarylazidoprazosin (IAAP) at high concentration, but it did not inhibit the photolabeling of ABCG2 with IAAP. Overall, we conclude that erlotinib reverses ABCB1- and ABCG2-mediated MDR in cancer cells through direct inhibition of the drug efflux function of ABCB1 and ABCG2. These findings may be useful for cancer combinational therapy with erlotinib in the clinic. [Cancer Res 2007;67(22):11012–20]

Introduction

The ATP-binding cassette (ABC) transporters are a superfamily of transmembrane proteins that transport a wide variety of substrates across extracellular and intracellular membranes, ranging from ions, sugars, amino acids, vitamins, lipids, and drugs to larger molecules such as oligosaccharides, oligopeptides, and even high molecular weight proteins (1). In the human genome, 48 different ABC transporters have been identified and divided into seven subfamilies (A–G) based on sequence similarities (2). The ABC transporters play a crucial role in the development of multidrug resistance (MDR). This occurs by pumping out drugs from the cells, and this process is coupled to the energy of ATP hydrolysis on the ATPase domain of ABC transporters that is stimulated in the presence of transport substrates (3). Thus far, the major members of the ABC transporters leading to MDR in cancer cells include ABC subfamily B member 1 (ABCB1; also called P-glycoprotein), MDR proteins (MRP; C subfamily of ABC transporters) and ABC subfamily G member 2 (ABCG2; breast cancer resistance protein/mitoxantrone resistance protein/placenta-specific ABC transporter; ref. 2). These proteins are highly varied transporters. They share the ability to recognize and transport a large number of structurally diverse, mainly hydrophobic, compounds from cells. However, each transporter can translocate unique compounds, in addition to their overlapping substrate specificity (2). Drugs transported by ABCB1 involve large hydrophobic, either uncharged or slightly positively charged, compounds, including most chemotherapeutic agents such as *Vinca* alkaloids, anthracyclines, epipodophyllotoxins, and taxanes (4). A few of MRPs subfamily members have been proved to confer MDR to organic anion compounds and phase II metabolic products including natural product chemotherapeutic agents, antifolates, and nucleotide analogues (5). The spectrum of chemotherapeutic agents transported by ABCG2 includes anthracyclines, mitoxantrone, camptothecin-derived and indolocarbazole topoisomerase I inhibitors, methotrexate, and flavopiridol (6).

The epidermal growth factor receptor (EGFR) is a transmembrane glycoprotein belonging to the ErbB/HER family of receptor tyrosine kinases, which homodimerize or heterodimerize on ligand activation, resulting in transphosphorylation of tyrosine residues in the cytoplasmic domain of tyrosine kinase receptors (7). In human tumors, the EGFR is often overexpressed, dysregulated, or mutated, and these abnormal alterations of EGFR activate a series of intracellular protein kinase signaling pathways such as the Ras/mitogenactivated protein kinase, phosphatidylinositol 3-kinase, signal transducer and activator of transcription, protein kinase C, and phospholipase D pathways, promoting tumor growth and progression including the promotion of proliferation, angiogenesis, invasion, and metastasis and inhibition of apoptosis (7, 8). Therefore, blockade of EGFR activation may be able to suppress cancer cell growth and progression. Presently, two predominant

Requests for reprints: Zhe-Sheng Chen, Department of Pharmaceutical Sciences, St. John's University, Jamaica, NY 11439. Phone: 718-990-1432; Fax: 718-990-1877; E-mail: Chenz@stjohns.edu or Li-Wu Fu, State Key Laboratory for Oncology in South China, Cancer Center, Sun Yat-Sen University, Guangzhou 510060, China. Phone: 86-20-873-431-63; Fax: 86-20-873-433-92; E-mail: Fulw@mail.sysu.edu.cn.

doi:10.1158/0008-5472.CAN-07-2686

classes of anti-EGFR targeting agents have been developed and used in the clinic. These include small-molecule tyrosine kinase inhibitors (TKI) that compete with ATP to bind to the intracellular receptor catalytic domain of EGFR, such as the 4-anilinoquinazoline derivatives gefitinib (Iressa, ZD1839) and erlotinib (Tarceva, OSI-774), and monoclonal antibodies such as cetuximab (Erbitux, C225) that block the ligand binding to the extracellular domain of EGFR and prevent receptor activation (9, 10).

Theoretically, TKIs usually are hydrophobic and need to enter the cell to reach their targets, allowing the ABC transporters to interact with them and modulate their effectiveness. The HER family TKI CI1033 (PD 183805), a 4-anilinoquinazoline derivative, enhances the cytotoxicity of topotecan and SN-38 through inhibition of ABCG2-mediated drug efflux in cancer cells (11). Gefitinib has been observed to directly inhibit the function of ABCB1 in multidrug resistant cancer cells (12) and to reverse ABCG2-mediated MDR *in vitro* (13–15). *In vivo* studies indicate that gefitinib modulates the function of ABCB1 and ABCG2, leading to increased oral absorption and reduced topotecan clearance (16), and enhances the antitumor activity and oral bioavailability of irinotecan in mice (17). It also increases the penetration of topotecan into brain extracellular fluid but decreases its ventricular cerebrospinal fluid penetration in a mouse model (18). Furthermore, gefitinib has a higher affinity for ABCG2 than ABCB1 or ABCC1 (19). However, there is no up-to-date report that elucidates the interaction in details between ABC transporters and erlotinib, which possesses a similar chemical structure to gefitinib. Therefore, we have examined the interaction between erlotinib and ABCB1, ABCC1, and ABCG2 in this study.

Materials and Methods

Materials. [^{3}H]Paclitaxel (37.9 Ci/mmol), [^{3}H]mitoxantrone (4 Ci/mmol), and [^{3}H]methotrexate (23 Ci/mmol) were purchased from Moravek Biochemicals, Inc. [^{3}H]$E_2$17βG (40.5 Ci/mmol) and [^{125}I]iodoarylazidoprazosin (IAAP; 2,200 Ci/mmol) were obtained from Perkin-Elmer Life Sciences. Monoclonal antibodies C219 (against ABCB1) and BXP-34 (against ABCG2) were acquired from Signet Laboratories, Inc. BXP-21 was obtained from Kamiya Biomedicals. Anti-actin monoclonal antibody was obtained from Santa Cruz Biotechnology, Inc. Erlotinib was kindly produced by OSI Pharmaceuticals. Fumitremorgin C was synthesized by Thomas McCloud Developmental Therapeutics Program, Natural Products Extraction Laboratory, National Cancer Institute, NIH. Other chemicals were purchased from Sigma Chemical Co.

Cell lines and cell culture. The ABCB1/P-glycoprotein–overexpressing drug-resistant cell line KB-C2 was established by step-by-step increases in the concentration of colchicine to parental human epidermoid carcinoma cell line KB-3-1 and was cultured in medium with 2 μg/mL colchicine (20). An ABCC1-overexpressing MDR cell line, KB-CV60, was also cloned from KB-3-1 cells and was maintained in medium with 1 μg/mL cepharanthine and 60 ng/mL vincristine (21). Both KB-C2 and KB-CV60 cells were kindly provided by Dr. Shin-ichi Akiyama. The wild-type ABCG2 [arginine (R) at 482 position]–overexpressing drug-resistant cell line MCF-7/Flv1000 was established by gradually increasing the concentration of flavopiridol to the parental drug-sensitive human breast cancer cell line MCF-7 and was cultured in medium with 1,000 nmol/L flavopiridol (22). HEK293/pcDNA3.1, ABCG2-482-G2, ABCG2-482-R5, and ABCG2-482-T7 cells were established by selection with G418 after transfecting HEK293 with either empty pcDNA3.1 or pcDNA3.1 vector containing full-length ABCG2 coding arginine (R), glycine (G), or threonine (T) at amino acid 482 position, and were cultured in medium with 2 mg/mL of G418 (23). All the cell lines were grown as adherent monolayers in flasks with DMEM (Hyclone Co.) containing 10% bovine serum at 37°C in a humidified atmosphere of 5% CO_2.

Preparation of membrane vesicles and total cell lysates. Membrane vesicles were prepared by the nitrogen cavitation method as previously described (24). Vesicles were stored at −80°C until ready for use. To prepare the total cell lysates, cells were harvested and rinsed twice with PBS. Cell extracts were prepared with radioimmunoprecipitation assay buffer (1 × PBS, 1% NP40, 0.5% sodium deoxycholate, 0.1% SDS, 100 μg/mL phenylmethylsulfonyl fluoride, 10 μg/mL aprotinin, 10 μg/mL leupeptin) for 30 min with occasional rocking and clarified by centrifugation at 12,000 × *g* at 4°C for 15 min. The supernatant containing total cell lysates was stored at −80°C until ready for use. The protein concentration was determined by the Bradford method. High Five insect cells (Invitrogen) were infected with the recombinant baculovirus carrying the human MDR1 or ABCG2 cDNAs with a His_6 tag at the COOH-terminal end [BV-MDR1(His_6) or BV-ABCG2(His_{10})] as described previously (25). The membrane vesicles of High Five insect cells were prepared as previously described (26) and stored at −70°C.

Western blot analysis. Identical amounts of total cell lysates (50 μg) or membrane vesicles (15 μg) were resolved by SDS-PAGE and electrophoretically transferred onto polyvinylidene fluoride (PVDF) membranes. After being incubated in blocking solution in TBST buffer [10 mmol/L Tris-HCl (pH 8.0), 150 mmol/L NaCl, and 0.1% Tween 20] for 1 h at room temperature, the membranes were immunoblotted overnight with primary monoclonal antibodies against ABCB1 or actin at 1:200 dilution or ABCG2 at 1:500 dilution at 4°C and were then incubated overnight at 4°C with horseradish peroxidase (HRP)–conjugated secondary antibody (1:1,000 dilution). The protein-antibody complex was detected by chemoluminescence. The protein expression was quantified by Scion Image software (Scion Co.).

3-(4,5-Dimethylthiazol-2-yl)-2,5-diphenyltetrazolium bromide cytotoxicity assay. Cells were harvested with trypsin and resuspended at a final concentration of 4 × 10^4/mL for KB-3-1 and 7.5 × 10^4/mL for all other cell lines. Aliquots (160 μL) for each cell suspension were distributed evenly into 96-well multiplates. For reversal experiments, different concentrations of chemotherapeutic drugs (20 μL/well) were added into designated wells after erlotinib, verapamil, or fumitremorgin C (20 μL/well) was added. After 68 h, 20 μL of 3-(4,5-dimethylthiazol-2-yl)-2,5-diphenyltetrazolium bromide (MTT) solution (4 mg/mL) were added to each well, and the plate was further incubated for 4 h, allowing viable cells to change the yellow MTT into dark-blue formazan crystals. Subsequently, the medium was discarded, and 100 μL of DMSO were added into each well to dissolve the formazan crystals. The absorbance in individual wells was determined at 570 nm with an OPSYS microplate Reader from DYNEX Technologies, Inc. The IC_{50} values were calculated from survival curves using the Bliss method (27).

Paclitaxel and mitoxantrone accumulation. The accumulation of paclitaxel in KB-3-1 and KB-C2 cells was measured with [^{3}H]paclitaxel as previously described (28), and the accumulation of mitoxantrone in ABCG2 related cells were measured with [^{3}H]mitoxantrone. The confluent cells in 24-well plates were preincubated with or without the reversal agents for 1 h at 37°C. To measure drug accumulation, the cells were then incubated with 0.1 μmol/L [^{3}H]paclitaxel or 0.2 μmol/L [^{3}H]mitoxantrone for 2 h in the presence or absence of the reversal agents at 37°C. After washing thrice with ice-cold PBS, the cells were trypsinized and lysed in 10 mmol/L lysis buffer (pH 7.4; containing 1% Triton X-100 and 0.2% SDS). Each sample was placed in scintillation fluid and radioactivity was measured in a Packard TRI-CARB 1900CA liquid scintillation analyzer from Packard Instrument Co., Inc.

***In vitro* transport assays.** Transport assays were done essentially using the rapid filtration method as previously described (29). Assays were carried out at 37°C for 10 min in a total volume of 50-μL medium [10 μg membrane vesicles, 0.25 mol/L sucrose, 10 mmol/L Tris-HCl (pH 7.4), 10 mmol/L $MgCl_2$, 4 mmol/L ATP or AMP, 10 mmol/L phosphocreatine, 100 μg/mL creatine phosphokinase, and 0.25 μmol/L [^{3}H]$E_2$17βG or 0.5 μmol/L [^{3}H]methotrexate]. Reactions were stopped by the addition of 3-mL ice-cold stop solution [0.25 mol/L sucrose, 100 mmol/L NaCl, and 10 mmol/L Tris-HCl (pH 7.4)]. For the rapid filtration step, samples were passed through 0.22-μm GVWP filters (Millipore Corp.) presoaked in the stop solution. The filters were washed thrice with 3-mL ice-cold stop solution. Radioactivity was measured

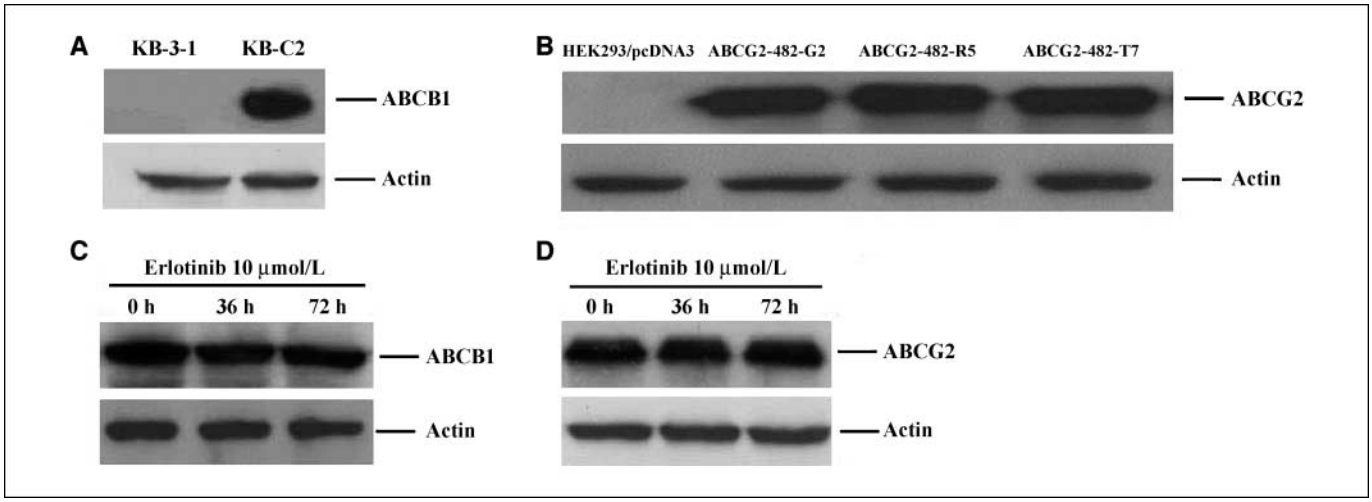

Figure 1. *A* and *B,* expression of ABCB1 and ABCG2 in cells. Equal amounts (15 μg protein) of membrane vesicles were used for each sample. *C* and *D,* effect of erlotinib on the expression of ABCB1 and ABCG2. KB-C2 and MCF-7/Flv1000 cells were treated with erlotinib at 10 μmol/L for 36 and 72 h. Equal amounts (50 μg protein) of total cell lysates were used for each sample. All samples were separated by SDS-PAGE and then transferred onto PVDF membrane. The membranes were immunoblotted with primary antibodies against ABCB1 or actin at 1:200 dilution or ABCG2 at 1:500 dilution at 4°C overnight, then incubated with HRP-conjugated secondary antibody at 1:1,000 dilution at 4°C overnight. Protein-antibody complex was detected by chemoluminescence. Results from a representative experiment; similar results were obtained in two other trials.

by the use of a liquid scintillation counter. For inhibition experiments, membrane vesicles were incubated with various concentrations of drugs for 1 h on ice, and then transport reactions were carried out for 10 min at 37°C in uptake medium containing 4 mmol/L ATP.

ATPase assay of ABCB1 and ABCG2. The Vi-sensitive ATPase activity of ABCB1 and ABCG2 in membrane vesicles of High Five insect cells was measured as previously described (30). The membrane vesicles (10 μg of protein) were incubated in ATPase assay buffer [50 mmol/L MES (pH 6.8), 50 mmol/L KCl, 5 mmol/L sodium azide, 2 mmol/L EGTA, 2 mmol/L DTT, 1 mmol/L ouabain, and 10 mmol/L $MgCl_2$] with or without 0.3 mmol/L vanadate at 37°C for 5 min, then incubated with different concentrations of drugs at 37°C for 3 min. The ATPase reaction was induced by the addition of 5 mmol/L MgATP, and the total volume was 0.1 mL. After incubation at 37°C for 20 min, the reactions were stopped by the addition of 0.1-mL 5% SDS solution. The liberated inorganic phosphate (P_i) was measured as described (30).

Photoaffinity labeling of ABCB1 and ABCG2 with [^{125}I]IAAP. The photoaffinity labeling of ABCB1 and ABCG2 with [^{125}I]IAAP was done as previously described (31). We have used the crude membranes from MCF-7/Flv1000 cells expressing R482 ABCG2 and membrane vesicles of High Five insect cells expressing ABCB1 for photolabeling experiments. The membranes (50 μg of protein) were incubated at room temperature with different concentrations of drugs in the ATPase assay buffer with [^{125}I]IAAP (7 nmol/L) for 5 min under subdued light. The samples were photo-cross-linked with 365-nm UV light for 10 min at room temperature. ABCG2 was immunoprecipitated with BXP-21 antibody (32) whereas ABCB1 was immunoprecipitated as described previously except that C219 antibody was used (33). The samples were electrophoresed on SDS-PAGE in a 7% Tris-acetate NuPAGE gel; the gels were dried and exposed to Bio-Max MR film (Eastman Kodak Co.) at −70°C for 8 to 12 h. The radioactivity incorporated into ABCB1 or ABCG2 band was quantified using the STORM 860 PhosphorImager system and ImageQuaNT (Molecular Dynamics).

Statistical analysis. All experiments were repeated at least two to three times and the differences were determined by using the Student *t* test. The significance was determined at $P < 0.05$.

Results

Erlotinib potentiates the sensitivity of anticancer drugs in the ABCB1- and ABCG2-overexpressing cells. To investigate the effect of erlotinib-induced reversal of ABCB1-, ABCG2-, and ABCC1-mediated MDR in cancer cells, we first examined the cytotoxicity of erlotinib in all cell lines by using the MTT assay. Erlotinib was not toxic to all cell lines used in this study (the IC_{50} values were all >50 μmol/L; data not shown), and erlotinib at 10 μmol/L showed no cytotoxicity in any of the cell lines. Therefore, 10 μmol/L was used as the highest reversal concentration of erlotinib. Second, we determined whether erlotinib could potentiate the sensitivity of chemotherapeutic drugs in ABCB1-overexpressing MDR cancer cells. The levels of ABCB1 expression in KB-3-1 and KB-C2 cells are shown in Fig. 1*A*, and the IC_{50} values of chemotherapeutic agents in both cell lines in the presence or absence of erlotinib are shown in Table 1. Compared with the parental KB-3-1 cells, KB-C2 cells showed high resistance to colchicine, vinblastine, and paclitaxel, which are all substrates of ABCB1. Erlotinib at 2.5 μmol/L slightly decreased the IC_{50} values of colchicine, vinblastine, and paclitaxel in KB-C2 cells and partially reversed their resistance; contrastingly, erlotinib at 10 μmol/L lowered these values more significantly and reversed most of their resistance. In the parental KB-3-1 cells, the IC_{50} values of colchicine, vinblastine, and paclitaxel in the presence or absence of erlotinib showed no significant difference. The reversal effect of erlotinib at 10 μmol/L in KB-C2 cells was a little weaker than that of verapamil at 10 μmol/L, but verapamil at 10 μmol/L also enhanced the cytotoxicity in KB-3-1 cells a little more. However, KB-3-1 and KB-C2 cells were equally sensitive to the non-ABCB1 substrate cisplatin, and this was not affected by erlotinib. Next, the reversal effect of erlotinib on ABCC1 (MRP1)-mediated MDR was determined. In KB-CV60 cells, erlotinib at 10 μmol/L did not reduce the IC_{50} value of vincristine (a substrate of ABCC1) and did not significantly reduce vincristine resistance (data not shown). Recent studies have shown that mutations at amino acid 482 in ABCG2 affect the substrate and antagonist specificity of ABCG2 (23, 34); therefore, we investigated the reversal effect of erlotinib on both wild-type (R482) and mutated (R482G and R482T) ABCG2–mediated MDR. The levels of ABCG2 expression in HEK293/pcDNA3, ABCG2-482-G2, ABCG2-482-R5, and ABCG2-482-T7 cells

are shown in Fig. 1*B*. As shown in Table 2, the IC_{50} values of flavopiridol, mitoxantrone, and SN-38 in three ABCG2-transfected cell lines, ABCG2-482-R5, ABCG2-482-G2, and ABCG2-482-T7, were higher than those in their parental cell line HEK293/pcDNA3. Erlotinib at 2.5 and 10 μmol/L mostly reduced the IC_{50} values of flavopiridol, mitoxantrone, and SN-38 and reversed their resistance in either wild-type or mutated ABCG2–overexpressing cells, and the reversal effects of erlotinib at 10 μmol/L were similar with the reversal effects of a known specific ABCG2 inhibitor, fumitremorgin C, at 2.5 μmol/L. In HEK293/pcDNA3 cells, the IC_{50} values of flavopiridol, mitoxantrone, and SN-38 in the presence or absence of erlotinib showed no significant difference (Table 2). Meanwhile, erlotinib did not alter the IC_{50} values of cisplatin, which is not a substrate of ABCG2 in all cell lines. These results suggest that erlotinib specifically potentiates the sensitivity of ABCB1 substrates in the ABCB1-overexpressing cells and also enhances the sensitivity of ABCG2 substrates in both wild-type and R482G/T mutant ABCG2–overexpressing cells we tested.

Erlotinib increases the accumulation of [^{3}H]paclitaxel or [^{3}H]mitoxantrone in the ABCB1- or ABCG2-overexpressing cells. To determine the effect of erlotinib on the function of ABCB1, we measured the accumulation of [^{3}H]paclitaxel in the presence or absence of erlotinib in KB-3-1 and KB-C2 cell lines. The results of the accumulation of [^{3}H]paclitaxel are shown in Fig. 2*A*. The levels of intracellular [^{3}H]paclitaxel in KB-C2 cells were ~25% of that in KB-3-1 cells. Erlotinib at 10 μmol/L increased the intracellular accumulation of [^{3}H]paclitaxel in KB-C2 cells to levels ~3.5-fold higher and this effect was comparable to that of 10 μmol/L verapamil. Neither erlotinib nor verapamil alters the intracellular accumulation of [^{3}H]paclitaxel in the parental KB-3-1 cells (Fig. 2*A*). Subsequently, we examined the accumulation of [^{3}H]mitoxantrone in ABCG2-overexpressing cells and their parental cells. As depicted in Fig. 2*B*, in all ABCG2-overexpressing cells, erlotinib, at 2.5 and 10 μmol/L, concentration-dependently increased the intracellular accumulation of [^{3}H]mitoxantrone, and the effects of erlotinib at 10 μmol/L were almost to the same extent as fumitremorgin C at 2.5 μmol/L. However, erlotinib did not significantly alter the intracellular accumulation of [^{3}H]mitoxantrone in HEK293/pcDNA3 cells. These data suggested that erlotinib might directly inhibit the drug efflux function of ABCB1 and ABCG2, resulting in the increase of the intracellular accumulation of [^{3}H]paclitaxel and [^{3}H]mitoxantrone.

Erlotinib does not alter the expression of ABCB1 and ABCG2. The reversal of ABCB1- and ABCG2-mediated MDR can be achieved either by decreasing ABCB1 and ABCG2 expression or by inhibiting their activities. To study the effect of erlotinib on ABCB1 and ABCG2 expression, we incubated KB-C2 and MCF-7/Flv1000 cells with erlotinib at 10 μmol/L for 36 and 72 h. The results of Western blot are shown in Fig. 1*C* and *D*, indicating that the protein levels of ABCB1 in KB-C2 cells and ABCG2 in MCF-7/Flv1000 cells were not altered by 10 μmol/L erlotinib treatment. This experiment suggests that erlotinib does not affect the expression of ABCB1 and ABCG2 for 3-day treatment of MDR cancer cells.

Erlotinib inhibits the transport of $E_2$17βG and methotrexate by ABCG2. ABCG2 is an ATP-dependent membrane efflux pump, which is able to transport several anticancer drugs or their metabolized production, leading to drug resistance. To investigate the effect of erlotinib on the transport activity of ABCG2, we used

Table 1. Effect of erlotinib and verapamil reversing ABCB1-mediated resistance to colchicine, vinblastine, paclitaxel, and cisplatin

Compounds	IC_{50} ± SD* (μmol/L)	
	KB-3-1	KB-C2
Colchicine	0.0073 ± 0.0010 (1.0)†	7.2584 ± 0.1987 (994.3)
+ Erlotinib 2.5 μmol/L	0.0072 ± 0.0007 (1.0)	5.6850 ± 0.3598 (778.8)
+ Erlotinib 10 μmol/L	0.0069 ± 0.0001 (0.9)	0.2564 ± 0.0110 (35.1)
+ Verapamil 10 μmol/L	0.0062 ± 0.0003 (0.8)	0.1143 ± 0.0022 (15.7)
Vinblastine	0.0437 ± 0.0011 (1.0)†	0.2716 ± 0.0033 (6.2)
+ Erlotinib 2.5 μmol/L	0.0416 ± 0.0015 (1.0)	0.1333 ± 0.0092 (3.1)
+ Erlotinib 10 μmol/L	0.0408 ± 0.0004 (0.9)	0.0676 ± 0.0030 (1.5)
+ Verapamil 10 μmol/L	0.0388 ± 0.0010 (0.9)	0.0394 ± 0.0038 (0.9)
Paclitaxel	0.0080 ± 0.0011 (1.0)†	5.1783 ± 2.2673 (647.3)
+ Erlotinib 2.5 μmol/L	0.0082 ± 0.0004 (1.0)	2.1966 ± 0.0564 (274.6)
+ Erlotinib 10 μmol/L	0.0086 ± 0.0006 (1.1)	0.0379 ± 0.0037 (4.7)
+ Verapamil 10 μmol/L	0.0070 ± 0.0018 (0.9)	0.0162 ± 0.0046 (2.0)
Cisplatin	1.9032 ± 0.0709 (1.0)†	1.7877 ± 0.2171 (0.9)
+ Erlotinib 2.5 μmol/L	1.8964 ± 0.1892 (1.0)	1.7400 ± 0.0697 (0.9)
+ Erlotinib 10 μmol/L	1.8507 ± 0.0305 (1.0)	1.7529 ± 0.0721 (0.9)
+ Verapamil 10 μmol/L	1.8246 ± 0.1105 (1.0)	1.6861 ± 0.0494 (0.9)

NOTE: Cell survival was determined by MTT assay as described in Materials and Methods.
*Data are the mean ± SD of at least three independent experiments done in triplicate.
† Fold resistance was the values of IC_{50} for colchicine, vinblastine, paclitaxel, and cisplatin of KB-3-1 cells in the presence of either erlotinib or verapamil, or KB-C2 cells with or without the reversing agents, divided by the IC_{50} values for colchicines, vinblastine, paclitaxel, and cisplatin of KB-3-1 cells without the reversing agents.

Table 2. Effect of erlotinib and fumitremorgin C reversing ABCG2-mediated resistance to flavopiridol, mitoxantrone, SN-38, and cisplatin in ABCG2 cDNA–transfected cell lines

Compounds	IC_{50} ± SD* (μmol/L)			
	HEK293/pcDNA3	ABCG2-482-G2	ABCG2-482-R5	ABCG2-482-T7
Flavopiridol	0.1640 ± 0.0171 (1.0)†	0.3976 ± 0.0910 (2.4)	0.2821 ± 0.0148 (1.7)	0.7578 ± 0.0423 (4.6)
+ Erlotinib 2.5 μmol/L	0.1153 ± 0.0083 (0.7)	0.1837 ± 0.0025 (1.1)	0.2095 ± 0.0366 (1.3)	0.2900 ± 0.0011 (1.8)
+ Erlotinib 10 μmol/L	0.1259 ± 0.0113 (0.8)	0.1291 ± 0.0091 (0.8)	0.1701 ± 0.0052 (1.0)	0.2497 ± 0.0704 (1.5)
+ FTC 2.5 μmol/L	0.1276 ± 0.0033 (0.8)	0.0988 ± 0.0386 (0.6)	0.1643 ± 0.0236 (1.0)	0.1643 ± 0.0296 (1.0)
Mitoxantrone	0.0356 ± 0.0030 (1.0)†	1.1042 ± 0.6023 (31.0)	0.4574 ± 0.3924 (12.8)	0.8424 ± 0.1858 (23.7)
+ Erlotinib 2.5 μmol/L	0.0318 ± 0.0025 (0.9)	0.2385 ± 0.0733 (6.l)	0.2257 ± 0.0524 (6.3)	0.1401 ± 0.0163 (3.9)
+ Erlotinib 10 μmol/L	0.0257 ± 0.0006 (0.7)	0.0685 ± 0.0083 (1.9)	0.0977 ± 0.0254 (2.7)	0.0647 ± 0.0089 (1.8)
+ FTC 2.5 μmol/L	0.0315 ± 0.0092 (0.9)	0.0696 ± 0.0054 (2.0)	0.0420 ± 0.0156 (1.2)	0.0919 ± 0.0208 (2.6)
SN-38	0.0058 ± 0.0002 (1.0)†	0.2042 ± 0.1362 (35.2)	0.1282 ± 0.0882 (22.1)	0.1171 ± 0.0704 (20.2)
+ Erlotinib 2.5 μmol/L	0.0049 ± 0.0014 (0.8)	0.0309 ± 0.0054 (5.3)	0.0183 ± 0.0021 (3.1)	0.0112 ± 0.0017 (1.9)
+ Erlotinib 10 μmol/L	0.0037 ± 0.0002 (0.6)	0.0068 ± 0.0009 (1.2)	0.0122 ± 0.0016 (2.1)	0.0092 ± 0.0008 (1.6)
+ FTC 2.5 μmol/L	0.0036 ± 0.0092 (0.8)	0.0050 ± 0.0009 (0.9)	0.0081 ± 0.0051 (1.4)	0.0082 ± 0.0023 (1.4)
Cisplatin	1.6300 ± 0.1697 (1.0)†	1.2305 ± 0.0841 (0.8)	1.3265 ± 0.2001 (0.8)	1.8435 ± 0.0233 (1.1)
+ Erlotinib 2.5 μmol/L	1.9785 ± 0.0262 (1.2)	1.1396 ± 0.3257 (0.7)	1.3055 ± 0.3005 (0.8)	1.9845 ± 0.1591 (1.2)
+ Erlotinib 10 μmol/L	1.8520 ± 0.0042 (1.1)	1.2191 ± 0.0728 (0.7)	1.2550 ± 0.3366 (0.8)	1.6570 ± 0.3521 (1.0)
+ FTC 2.5 μmol/L	1.1535 ± 0.0488 (0.7)	1.0466 ± 0.0280 (0.6)	1.3495 ± 0.2072 (0.8)	1.9530 ± 0.0834 (1.2)

NOTE: Cell survival was determined by MTT assay as described in Materials and Methods.
Abbreviation: FTC, fumitremorgin C.
*Data are the mean ± SD of at least three independent experiments done in triplicate.
†Fold resistance was the IC_{50} values for flavopiridol, mitoxantrone, SN-38, and cisplatin of HEK293/pcDNA3 cells in the presence of either erlotinib or FTC, or the transfectant cells with or without the reversing agents, divided by the IC_{50} values for flavopiridol, mitoxantrone, SN-38, and cisplatin of HEK293/pcDNA3 cells without the reversing agents.

the membrane vesicles prepared from HEK293/pcDNA3, ABCG2-482-G2, ABCG2-482-R5, and ABCG2-482-T7 cells. First, the physiologic substrate $E_2$17βG was used as the transport substance of ABCG2. As shown in Fig. 3*A*, the rates of ATP-dependent uptake of $E_2$17βG were significantly different only in the membrane vesicles of ABCG2-482-R5 cells but not in the membrane vesicles of other cell lines. Subsequently, we carried out inhibition experiments using membrane vesicles prepared from HEK293/pcDNA3 and ABCG2-482-R5 cells. The effects of erlotinib on the transport of $E_2$17βG by ABCG2 are shown in Fig. 3*B*. The rates of $E_2$17βG uptake were significantly inhibited by erlotinib in a concentration-dependent manner, but the inhibition effect of erlotinib was a little weaker than that of fumitremorgin C. Second, the anticancer drug methotrexate was used as the transport substrate of ABCG2. We found that the transport results of methotrexate were consistent with those of $E_2$17βG. Similarly, the rates of ATP-dependent uptake of methotrexate were significantly different only in the membrane vesicles of ABCG2-482-R5 cells (Fig. 3*C*); the rates of methotrexate uptake were concentration-dependently inhibited by erlotinib; and the inhibition effect of erlotinib was weaker than that of fumitremorgin C (Fig. 3*D*). These transport results suggest that among the wild-type and variant ABCG2, only wild-type ABCG2 is able to ATP-dependently transport $E_2$17βG and methotrexate, and erlotinib inhibits the transport of $E_2$17βG and methotrexate by wild-type ABCG2.

Erlotinib activates the ATPase activity of ABCB1 and ABCG2. The drug efflux function of ABCB1 and ABCG2 is coupled to ATP hydrolysis, which is stimulated in the presence of ABCB1 and ABCG2 substrates. To assess the effect of erlotinib on the ATPase activity of ABCB1 and ABCG2, we measured the ABCB1- and ABCG2-mediated ATP hydrolysis using various concentrations of erlotinib under conditions that suppressed the activity of other major membrane ATPases. As shown in Fig. 4*A* and *B*, erlotinib concentration-dependently enhanced the ATPase activity of ABCB1 and ABCG2. Furthermore, the maximum stimulated ATPase activities of ABCB1 and ABCG2 by erlotinib were up to 76.70 and 104.15 nmol P_i/mg protein/min, respectively, and the concentrations of erlotinib required for 50% stimulation of ATPase activity of ABCB1 and ABCG2 were 4.93 and 0.17 μmol/L, respectively. These data indicate that erlotinib may be the substrate of ABCB1 and ABCG2, although the ABCB1- or ABCG2-expressing cells do not exhibit resistance to erlotinib, which is most likely because of the very low toxicity of this drug (IC_{50} >50 μmol/L).

Erlotinib differentially affects the photolabeling of ABCB1 and ABCG2 with [^{125}I]IAAP. ABCB1 and ABCG2 can be photolabeled by their transport substrate [^{125}I]IAAP, and their substrates as well as inhibitors can compete with [^{125}I]IAAP for binding to ABCB1 and ABCG2 (32). We examined the photolabeling of ABCB1 and ABCG2 with [^{125}I]IAAP by using the membrane vesicles in the presence of various concentrations of erlotinib to primarily understand the physical interaction of erlotinib with the substrate interaction sites of ABCB1 and ABCG2. As indicated in Fig. 4*C* and *D*, erlotinib only slightly inhibited the photoaffinity labeling of ABCB1 with [^{125}I]IAAP at a concentration of 100 μmol/L. However, 10 μmol/L cyclosporine A, an inhibitor of ABCB1, almost completely blocked the ABCB1 photolabeling of [^{125}I]IAAP, and verapamil at 20 μmol/L showed inhibition by up to 50%. Moreover,

erlotinib at 1 to 100 μmol/L did not affect the photolabeling of ABCG2 with [^{125}I]IAAP, but the ABCG2 inhibitor fumitremorgin C at 20 μmol/L decreased the ABCG2 photolabeling of [^{125}I]IAAP to ~50% of the control group. Therefore, these results suggest that erlotinib differentially affects the photolabeling of ABCB1 and ABCG2.

Discussion

Erlotinib is an orally available, potent, reversible, and selective small-molecule inhibitor of the EGFR tyrosine kinase (35). It has been reported that erlotinib (*a*) inhibits human EGFR tyrosine kinase, (*b*) reduces EGFR autophosphorylation in intact tumor cells with nmol/L IC_{50} values, and (*c*) blocks cell cycle progression in the G_1 phase and induces apoptosis (36). Based on a randomized double-blind, placebo-controlled phase III trial (37), erlotinib was approved by the Food and Drug Administration (FDA) in November 2004 for treatment of locally advanced or metastatic non–small-cell lung cancer after failure of at least one prior chemotherapy regimen. Most recently, the FDA approved erlotinib for use in combination with gemcitabine as first-line treatment of patients with locally advanced, unresectable, or metastatic pancreatic cancer based on the improvement of overall and progression-free survival in a phase III trial (38). Erlotinib is also under investigation in several other tumor types, including head and neck, breast, colon, and ovarian cancer, in combination with chemotherapy and other targeted therapies (35).

In the present study, we showed for the first time that erlotinib potentiated the sensitivity of established ABCB1 and ABCG2 substrates and increased the accumulation of paclitaxel or mitoxantrone in either ABCB1- or ABCG2-overexpressing cells. Furthermore, erlotinib did not alter the sensitivity of non-ABCB1 or non-ABCG2 substrates in all cells and also could not reverse ABCC1-mediated MDR. These data suggested that the reversal effect of erlotinib on MDR could be specific to ABCB1 and ABCG2. In addition, the results of ATPase analysis showed that erlotinib significantly enhanced the ATPase activity of both ABCB1 and ABCG2 in a concentration-dependent manner. A majority of substrates that interact with the ABC drug transporters stimulate the ATP hydrolysis, and the fact that the presence of erlotinib stimulated the ATP hydrolysis by both ABCB1 and ABCG2 suggested that it behaved similarly to the known substrates of these transporters. These data led us to speculate on the direct interaction of the compound with the transporters. Further experiments with either the radiolabeled erlotinib in an accumulation assay or the photoaffinity analogue of erlotinib in a binding assay would provide conclusive evidence for the direct interaction of erlotinib with these transporters. While this article was in preparation, a new publication suggested that erlotinib is the substrate of ABCG2 (39); this supports our above ATPase results.

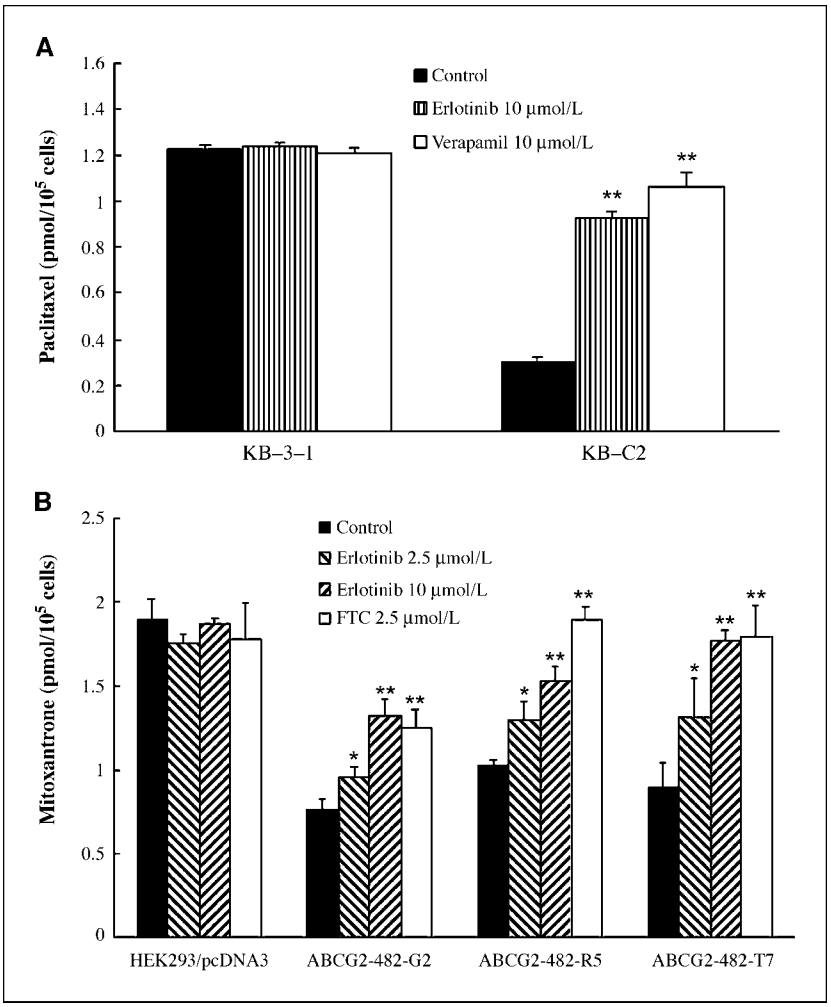

Figure 2. Effect of erlotinib on the accumulation of [^{3}H]paclitaxel and [^{3}H]mitoxantrone. The accumulation of [^{3}H]paclitaxel (*A*) or [^{3}H]mitoxantrone (*B*) was measured after cells were preincubated with or without erlotinib, verapamil, or fumitremorgin C (*FTC*) for 1 h at 37°C and then incubated with 0.1 μmol/L [^{3}H]paclitaxel or 0.02 μmol/L [^{3}H]mitoxantrone for another 2 h at 37°C. *Columns,* mean of triplicate determinations; *bars,* SD. *, $P < 0.05$; **, $P < 0.01$, versus the control group. Experiments were done at least three independent times, and a representative experiment is shown.

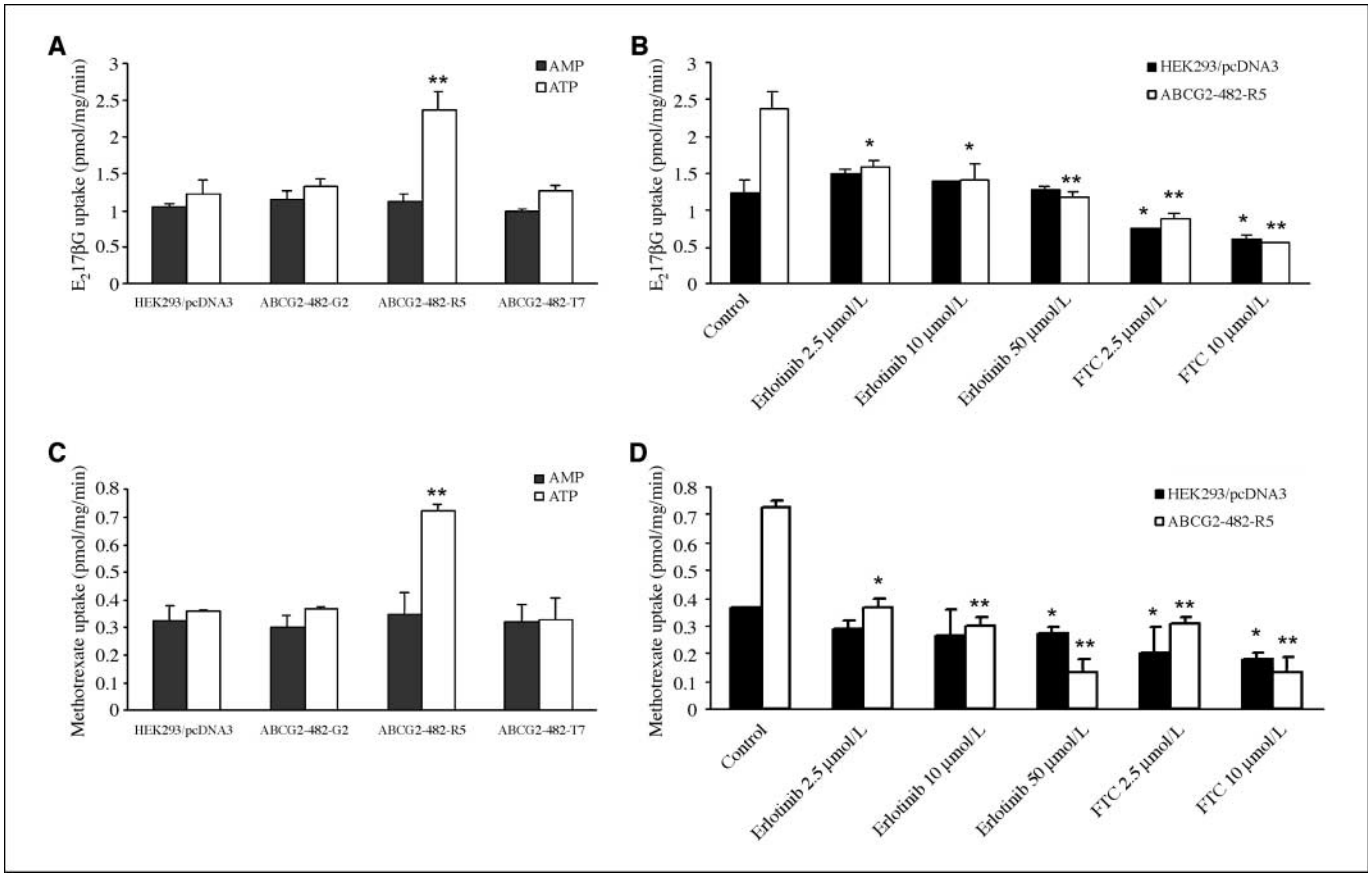

Figure 3. Effect of erlotinib on the transport of $E_2$17βG and methotrexate by ABCG2. Membrane vesicles (10 μg) were prepared from HEK293/pcDNA3, ABCG2-482-G2, ABCG2-482-R5, and ABCG2-482-T7 cells. The rates of the uptake of [^{3}H]$E_2$17βG (*A* and *B*) and [^{3}H]methotrexate (*MTX*; *C* and *D*) into membrane vesicles were measured for 10 min at 37°C in uptake medium containing 4 mmol/L of ATP or AMP. For inhibition experiments, membrane vesicles from HEK293/pcDNA3.1 and ABCG2-482-R5 cells were incubated with various concentrations of erlotinib or fumitremorgin C for 1 h on ice, and then transport reactions were carried out for 10 min at 37°C in uptake medium containing 4 mmol/L ATP. *Columns,* mean of triplicate determinations; *bars,* SD. *, $P < 0.05$; **, $P < 0.01$, versus the control group. Experiments were done at least three independent times, and a representative experiment is shown.

The *in vitro* concentrations of erlotinib used in our experiments are similar to those obtained in plasma after therapeutic treatment (40, 41). Therefore, the reversal effects shown in the present study would be sufficient for reversing ABCB1- and ABCG2-mediated drug resistance *in vivo*. However, the tissue distribution of ABCB1 and ABCG2 is very broad in the body. For example, ABCB1 is highly expressed in the adrenal and the kidney whereas ABCG2 is highly expressed in the placenta, liver, and intestine, and the blood-brain barrier expresses both ABCB1 and ABCG2 (2). Therefore, when the combination of erlotinib with ABCB1 and ABCG2 substrates is applied in the clinic, erlotinib may affect the plasma concentrations and tissue distribution of these drugs, resulting in adverse effects because erlotinib may also inhibit ABCB1- and ABCG2-mediated drug transport in normal cells. In fact, when the combination of gefitinib with camptothecins was used in mice, gefitinib was able to increase oral absorption of camptothecins, reduce topotecan clearance (16), enhance the oral bioavailability of irinotecan (17), and increase the topotecan brain extracellular fluid penetration while decreasing its ventricular cerebrospinal fluid penetration (18).

Interestingly, when the photolabeling of ABCB1 and ABCG2 with [^{125}I]IAAP was used to elucidate the binding site of erlotinib on the pumps, we found that erlotinib differentially affected the photoaffinity labeling of ABCB1 and ABCG2 with [^{125}I]IAAP. The results show that erlotinib slightly inhibited the photolabeling of ABCB1 at high concentrations but did not inhibit the photolabeling of ABCG2. However, these high concentrations of erlotinib are not physiologically relevant as the reported steady-state plasma concentration in patients after the recommended dose of 150 mg/d is 3 to 5 μmol/L (40). In our results of transport by ABCG2 vesicles, $E_2$17βG and methotrexate are only transported by the wild-type ABCG2 and not by the two mutated R482G and R482T ABCG2. This is consistent with our previous study (29) and provides an explanation for a recent finding that showed that among a panel of ABCG2-overexpressing drug-resistant cell lines, only the wild-type ABCG2–expressing cells had the ability to mediate methotrexate resistance (42). Furthermore, the transport of $E_2$17βG and methotrexate by ABCG2 is inhibited by erlotinib in a concentration-dependent manner. This provides direct evidence for the first time that the reversal effect of erlotinib on ABCB1- and ABCG2-mediated MDR is based on the inhibition of the transport function of these two pumps by erlotinib. The other evidence is that erlotinib had no effect on the expression levels of ABCB1 in KB-C2 cells and ABCG2 in MCF-7/Flv1000 cells. However, in this study, we did not examine and could not exclude the effects of erlotinib on the EGFR signaling pathway. Although the concentrations of erlotinib used in the current study were sufficient to block the EGFR signaling pathway, we did not observe any significant effect on the growth and survival of cells (data not shown).

Recently, Cusatis et al. (43) reported that one common functional single-nucleotide polymorphism in the ABCG2 gene, ABCG2 421C→A (Q141K), is associated with diarrhea, which is a gefitinib-induced adverse effect, and led to a high risk of diarrhea in patients treated with oral gefitinib. The same group also showed that this functional variant of ABCG2 is associated with greater gefitinib accumulation at steady state and may be relevant to the toxicity and antitumor activity of EGFR TKIs (39). These findings suggest that the functional variants of ABCB1 or ABCG2 in patients may affect the pharmacokinetics and pharmacodynamics not only of established ABCB1 and ABCG2 substrates such as camptothecins and mitoxantrone but also of novel molecular target anticancer drugs such as gefitinib. Therefore, these functional variants can cause alterations in the adverse events and therapeutic effects of chemotherapy. Similar to gefitinib, the most frequent adverse effects of erlotinib in patients are skin rash and diarrhea, whereas other side effects such as headache, mucositis, hyperbilirubinemia, neutropenia, and anemia are less common (35). Thus, these functional variants of ABCB1 or ABCG2 in patients may also affect the pharmacokinetics and pharmacodynamics of erlotinib, resulting in an attenuation of its adverse events and therapeutic effects.

In conclusion, the present study shows that erlotinib significantly reverses ABCB1- and ABCG2-mediated MDR in cancer cells by directly inhibiting the drug efflux function of ABCB1 and ABCG2, resulting in the increase of the intracellular accumulation of the anticancer drugs. The mechanistic study found that erlotinib stimulated the ATPase activity of these two pumps but did not inhibit the photoaffinity labeling of the transporters with [^{125}I]IAAP. Both our current and previous studies showed that gefitinib reverses ABCB1- and ABCG2-mediated MDR, indicating

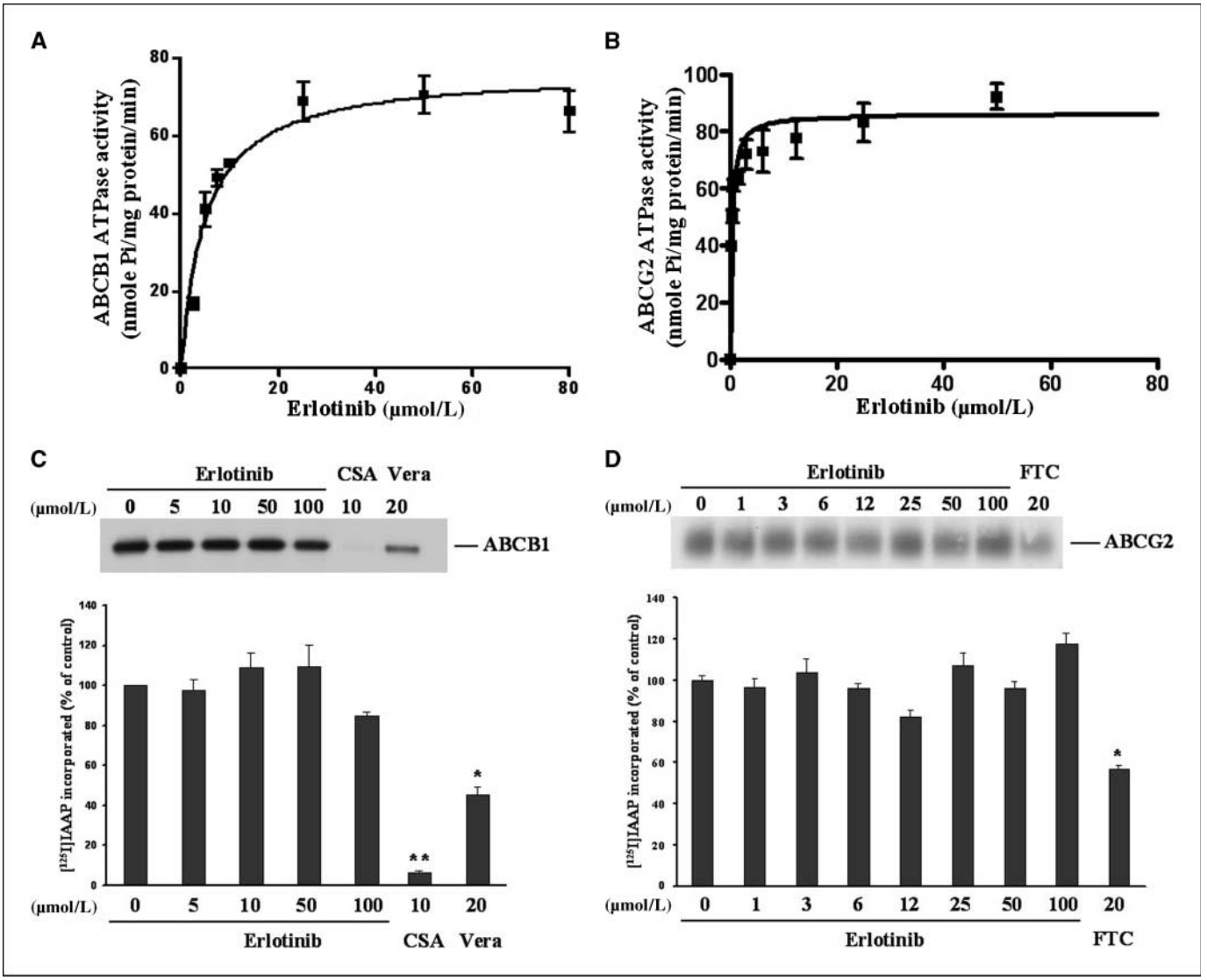

Figure 4. Effect of erlotinib on the ATPase activity and [^{125}I]IAAP photoaffinity labeling of ABCB1 and ABCG2. The Vi-sensitive ATPase activity of ABCB1 (*A*) and ABCG2 (*B*) in membrane vesicles was determined with different concentrations of erlotinib, as described in Materials and Methods. The basal ATPase activity (in the absence of erlotinib) was subtracted from the activities obtained at the indicated erlotinib concentrations and the graph was fitted by nonlinear least-squares regression analysis using GraphPad Prism version 2.0. *Points,* mean from at least three independent experiments; *bars,* SE. The photoaffinity labeling of ABCB1 and ABCG2 with [^{125}I]IAAP was done with different concentrations of erlotinib. The radioactivity incorporated into ABCB1 and ABCG2 was determined by exposing the gel to an X-ray film at −70°C. *C* and *D,* autoradiograms and quantification of incorporation of IAAP into ABCB1 and ABCG2 bands, respectively, from at least two independent experiments. Cyclosporine A, verapamil, and fumitremorgin C were used as the positive controls for photolabeling of ABCB1 and ABCG2 by [^{125}I]IAAP. *CSA,* cyclosporine A; *Vera,* verapamil. *, $P < 0.05$; **, $P < 0.01$, versus the control group.

that this class of TKIs may have the common function of reversing ABCB1- and ABCG2-mediated MDR. Consequently, our results support the fact that it is optimal to use the strategies of combining established ABCB1 and ABCG2 substrate anticancer drugs with this class of TKIs in patients.

Acknowledgments

Received 7/16/2007; revised 8/27/2007; accepted 9/20/2007.

Grant support: St. John's University Tenure Track Faculty Start-Up Funding, no. C-0531 (Z-S. Chen); the Chinese Ministry of Education Doctor Foundation, no. 20050558062 (L-W. Fu); the Guangdong Provincial Key Sciences Foundation, no. 2004B30101005 (L-W. Fu); the Intramural Research Program, Center for Cancer Research, National Cancer Institute, NIH (W-I. Kim, S. Shukla, R.W. Robey, S.E. Bates, and S.V. Ambudkar); and Kaisi fellowship for overseas study at St. John's University from Sun Yat-Sen University (Z. Shi).

The costs of publication of this article were defrayed in part by the payment of page charges. This article must therefore be hereby marked *advertisement* in accordance with 18 U.S.C. Section 1734 solely to indicate this fact.

We thank Dr. Michael M. Gottesman (National Cancer Institute, NIH, Bethesda, MD) for KB-3-1 cells, Dr. Shin-ichi Akiyama (Kagoshima University, Kagoshima, Japan) for KB-C2 and KB-CV60 cell lines, Yangmin (Mimi) Chen (Montgomery High School, New Jersey) for editorial assistance, the members of Cancer Chemotherapy laboratory (Z-S. Chen) for helpful discussions and review of the manuscript, and OSI Pharmaceuticals (Melville, NY) for providing erlotinib.

References

1. Higgins CF. ABC transporters: from microorganisms to man. Annu Rev Cell Biol 1992;8:67–113.
2. Dean M, Rzhetsky A, Allikmets R. The human ATP-binding cassette (ABC) transporter superfamily. Genome Res 2001;11:1156–66.
3. Ambudkar SV, Dey S, Hrycyna CA, Ramachandra M, Pastan I, Gottesman MM. Biochemical, cellular, and pharmacological aspects of the multidrug transporter. Annu Rev Pharmacol Toxicol 1999;39:361–98.
4. Ambudkar SV, Kimchi-Sarfaty C, Sauna ZE, Gottesman MM. P-glycoprotein: from genomics to mechanism. Oncogene 2003;22:7468–85.
5. Kruh GD, Belinsky MG. The MRP family of drug efflux pumps. Oncogene 2003;22:7537–52.
6. Doyle LA, Ross DD. Multidrug resistance mediated by the breast cancer resistance protein BCRP (ABCG2). Oncogene 2003;22:7340–58.
7. Normanno N, De Luca A, Bianco C, et al. Epidermal growth factor receptor (EGFR) signaling in cancer. Gene 2006;366:2–16.
8. Grant S, Qiao L, Dent P. Roles of ERBB family receptor tyrosine kinases, and downstream signaling pathways, in the control of cell growth and survival. Front Biosci 2002;7:d376–89.
9. Cascone T, Morelli MP, Ciardiello F. Small molecule epidermal growth factor receptor (EGFR) tyrosine kinase inhibitors in non-small cell lung cancer. Ann Oncol 2006;17 Suppl 2:ii46–8.
10. Grunwald V, Hidalgo M. Developing inhibitors of the epidermal growth factor receptor for cancer treatment. J Natl Cancer Inst 2003;95:851–67.
11. Erlichman C, Boerner SA, Hallgren CG, et al. The HER tyrosine kinase inhibitor CI1033 enhances cytotoxicity of 7-ethyl-10-hydroxycamptothecin and topotecan by inhibiting breast cancer resistance protein-mediated drug efflux. Cancer Res 2001;61:739–48.
12. Kitazaki T, Oka M, Nakamura Y, et al. Gefitinib, an EGFR tyrosine kinase inhibitor, directly inhibits the function of P-glycoprotein in multidrug resistant cancer cells. Lung Cancer 2005;49:337–43.
13. Nakamura Y, Oka M, Soda H, et al. Gefitinib ("Iressa," ZD1839), an epidermal growth factor receptor tyrosine kinase inhibitor, reverses breast cancer resistance protein/ABCG2-mediated drug resistance. Cancer Res 2005;65:1541–6.
14. Yanase K, Tsukahara S, Asada S, Ishikawa E, Imai Y, Sugimoto Y. Gefitinib reverses breast cancer resistance protein-mediated drug resistance. Mol Cancer Ther 2004;3:1119–25.
15. Yang CH, Huang CJ, Yang CS, et al. Gefitinib reverses chemotherapy resistance in gefitinib-insensitive multidrug resistant cancer cells expressing ATP-binding cassette family protein. Cancer Res 2005;65:6943–9.
16. Leggas M, Panetta JC, Zhuang Y, et al. Gefitinib modulates the function of multiple ATP-binding cassette transporters *in vivo*. Cancer Res 2006;66:4802–7.
17. Stewart CF, Leggas M, Schuetz JD, et al. Gefitinib enhances the antitumor activity and oral bioavailability of irinotecan in mice. Cancer Res 2004;64:7491–9.
18. Zhuang Y, Fraga CH, Hubbard KE, et al. Topotecan central nervous system penetration is altered by a tyrosine kinase inhibitor. Cancer Res 2006;66:11305–13.
19. Ozvegy-Laczka C, Hegedus T, Varady G, et al. High-affinity interaction of tyrosine kinase inhibitors with the ABCG2 multidrug transporter. Mol Pharmacol 2004;65:1485–95.
20. Akiyama S, Fojo A, Hanover JA, Pastan I, Gottesman MM. Isolation and genetic characterization of human KB cell lines resistant to multiple drugs. Somat Cell Mol Genet 1985;11:117–26.
21. Taguchi Y, Yoshida A, Takada Y, Komano T, Ueda K. Anti-cancer drugs and glutathione stimulate vanadate-induced trapping of nucleotide in multidrug resistance-associated protein (MRP). FEBS Lett 1997;401:11–4.
22. Robey RW, Medina-Perez WY, Nishiyama K, et al. Overexpression of the ATP-binding cassette half-transporter, ABCG2 (Mxr/BCrp/ABCP1), in flavopiridol-resistant human breast cancer cells. Clin Cancer Res 2001;7:145–52.
23. Robey RW, Honjo Y, Morisaki K, et al. Mutations at amino-acid 482 in the ABCG2 gene affect substrate and antagonist specificity. Br J Cancer 2003;89:1971–8.
24. Cornwell MM, Gottesman MM, Pastan IH. Increased vinblastine binding to membrane vesicles from multidrug-resistant KB cells. J Biol Chem 1986;261:7921–8.
25. Ramachandra M, Ambudkar SV, Chen D, et al. Human P-glycoprotein exhibits reduced affinity for substrates during a catalytic transition state. Biochemistry 1998;37:5010–9.
26. Kerr KM, Sauna ZE, Ambudkar SV. Correlation between steady-state ATP hydrolysis and vanadate-induced ADP trapping in Human P-glycoprotein. Evidence for ADP release as the rate-limiting step in the catalytic cycle and its modulation by substrates. J Biol Chem 2001;276:8657–64.
27. Shi Z, Liang YJ, Chen ZS, et al. Reversal of MDR1/P-glycoprotein-mediated multidrug resistance by vector-based RNA interference *in vitro* and *in vivo*. Cancer Biol Ther 2006;5:39–47.
28. Aoki S, Chen ZS, Higasiyama K, Setiawan A, Akiyama S, Kobayashi M. Reversing effect of agosterol A, a spongean sterol acetate, on multidrug resistance in human carcinoma cells. Jpn J Cancer Res 2001;92:886–95.
29. Chen ZS, Robey RW, Belinsky MG, et al. Transport of methotrexate, methotrexate polyglutamates, and 17β-estradiol 17-(β-D-glucuronide) by ABCG2: effects of acquired mutations at R482 on methotrexate transport. Cancer Res 2003;63:4048–54.
30. Ambudkar SV. Drug-stimulatable ATPase activity in crude membranes of human MDR1-transfected mammalian cells. Methods Enzymol 1998;292:504–14.
31. Sauna ZE, Ambudkar SV. Evidence for a requirement for ATP hydrolysis at two distinct steps during a single turnover of the catalytic cycle of human P-glycoprotein. Proc Natl Acad Sci U S A 2000;97:2515–20.
32. Shukla S, Robey RW, Bates SE, Ambudkar SV. The calcium channel blockers, 1,4-dihydropyridines, are substrates of the multidrug resistance-linked ABC drug transporter, ABCG2. Biochemistry 2006;45:8940–51.
33. Hrycyna CA, Ramachandra M, Pastan I, Gottesman MM. Functional expression of human P-glycoprotein from plasmids using vaccinia virus-bacteriophage T7 RNA polymerase system. Methods Enzymol 1998;292:456–73.
34. Honjo Y, Hrycyna CA, Yan QW, et al. Acquired mutations in the MXR/BCRP/ABCP gene alter substrate specificity in MXR/BCRP/ABCP-overexpressing cells. Cancer Res 2001;61:6635–9.
35. Arora A, Scholar EM. Role of tyrosine kinase inhibitors in cancer therapy. J Pharmacol Exp Ther 2005;315:971–9.
36. Moyer JD, Barbacci EG, Iwata KK, et al. Induction of apoptosis and cell cycle arrest by CP-358,774, an inhibitor of epidermal growth factor receptor tyrosine kinase. Cancer Res 1997;57:4838–48.
37. Shepherd FA, Rodrigues Pereira J, Ciuleanu T, et al. Erlotinib in previously treated non-small-cell lung cancer. N Engl J Med 2005;353:123–32.
38. Moore MJ, Goldstein D, Hamm J, et al. Erlotinib plus gemcitabine compared to gemcitabine alone in patients with advanced pancreatic cancer: a phase III trial of the National Cancer Institute of Canada Clinical Trials Group [NCIC-CTG] [abstract 1]. J Clin Oncol 2007;25:1960–6.
39. Li J, Cusatis G, Brahmer J, et al. Association of variant ABCG2 and the pharmacokinetics of epidermal growth factor receptor tyrosine kinase inhibitors in cancer patients. Cancer Biol Ther 2007;6:432–8.
40. Hidalgo M, Siu LL, Nemunaitis J, et al. Phase I and pharmacologic study of OSI-774, an epidermal growth factor receptor tyrosine kinase inhibitor, in patients with advanced solid malignancies. J Clin Oncol 2001;19:3267–79.
41. Ellis AG, Doherty MM, Walker F, et al. Preclinical analysis of the analinoquinazoline AG1478, a specific small molecule inhibitor of EGF receptor tyrosine kinase. Biochem Pharmacol 2006;71:1422–34.
42. Volk EL, Farley KM, Wu Y, Li F, Robey RW, Schneider E. Overexpression of wild-type breast cancer resistance protein mediates methotrexate resistance. Cancer Res 2002;62:5035–40.
43. Cusatis G, Gregorc V, Li J, et al. Pharmacogenetics of ABCG2 and adverse reactions to gefitinib. J Natl Cancer Inst 2006;98:1739–42.

Erlotinib (Tarceva, OSI-774) Antagonizes ATP-Binding Cassette Subfamily B Member 1 and ATP-Binding Cassette Subfamily G Member 2–Mediated Drug Resistance

Zhi Shi, Xing-Xiang Peng, In-Wha Kim, et al.

Cancer Res 2007;67:11012-11020.